

Supplementary Material

Figure S1: Effect of nicotine on the main phase transition temperature of DPPC multilamellar vesicles. Data is represented by the change of the DPPC main phase transition temperature in the absence ($T_{m,0}$) and presence (T_m) of nicotine, ($\Delta T_m/T_m = (T_m - T_{m,0})/T_m$), as a function of nicotine concentration. The analysis was based on the binding scheme proposed by Basso et al [1], which took into account the different binding constants of the drug to the gel and fluid lipid phases. The model states that the relative change in the phospholipid phase transition temperature ($\Delta T_m/T_m$) caused by drug binding is $\Delta T_m/T_m = -(RT_{m,0}/\Delta H_0)\ln[(1 + C_F[L]_{Tot})/(1 + C_G[L]_{Tot})]$, where ΔH_0 is the enthalpy change of pure DPPC, $[L]_{Tot}$ represents the total ligand concentration added into the sample solution, and C_F and C_G are fitting parameters that depend both on the partition constant of nicotine to the membrane and on the binding constants of the drug to the membrane gel (K_G) and fluid (K_F) phases. From the fitting, one can obtain the ratio of the binding constants as $K_F/K_G = C_F/C_G$. For nicotine in DPPC, K_F/K_G was determined as 1.7 ± 0.3 .

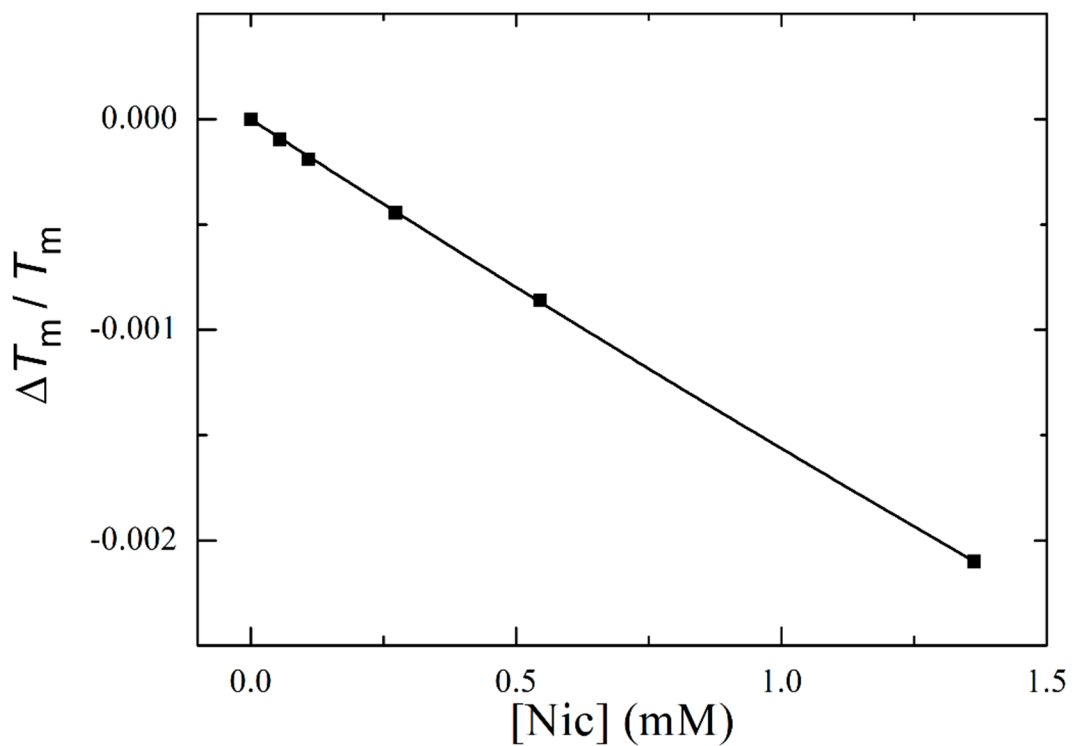


Figure S2: Nicotine structure and molecular abundance of charged states. (A) Molecular structure of nicotine along with the pKa values of the ionizable nitrogen moieties. (B) Molecular abundance of the neutral (NTN), monoprotonated (NTH), and diprotonated (NT2H) species of nicotine as a function of the pH. The distribution of the molecular species was modeled according to equations $pH = pK_a_1 - \log[molNic/molNic^{H^+}]$ and $pH = pK_a_2 - \log[molNic^{H^+}/molNic^{2H^+}]$ [2].

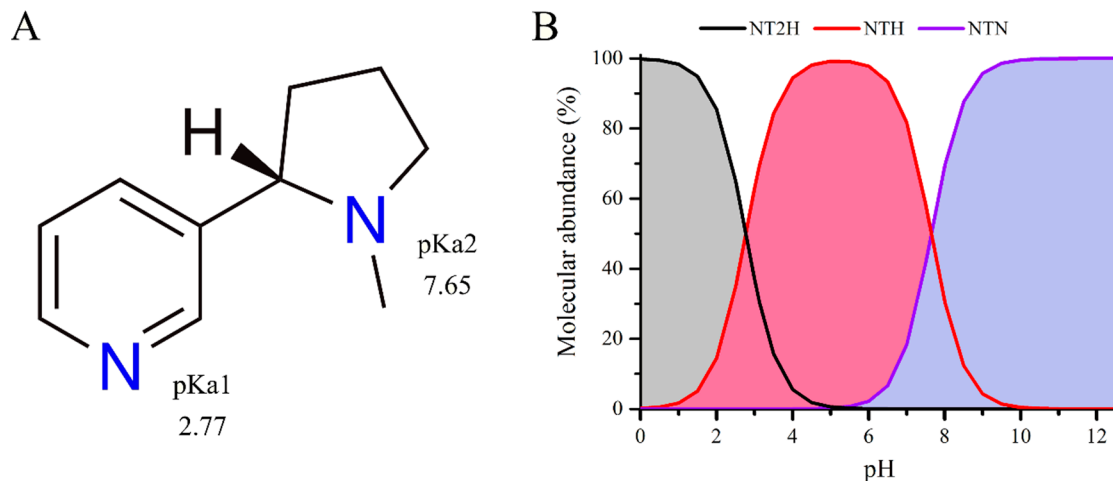


Figure S3: Analysis of the 5-PCSL ESR spectra in DPPC using parameters defined on the spectra. **(A)** Temperature dependence of the maximum hyperfine splitting ($2A_{max}$) in the absence and presence of 10 mol% of nicotine. The higher the $2A_{max}$ the more packed is the bilayer. **(B)** Temperature dependence of the linewidth of the middle line (ΔH_0) in the absence and presence of 10 mol% of nicotine. The narrower the ΔH_0 the higher the mobility of the spin label. The inset is a magnification of the 37 °C-to-44 °C interval.

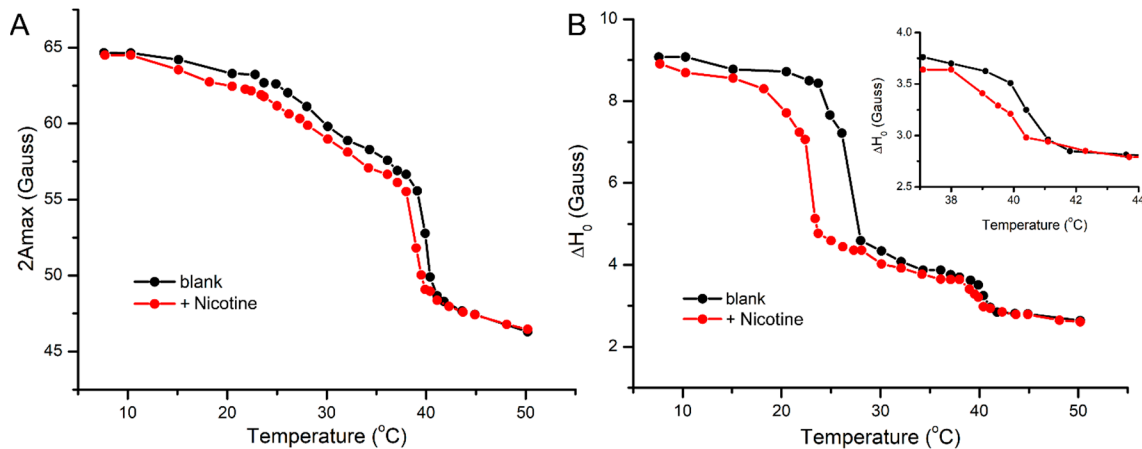


Figure S4: Two-component spectra in the gel phase of DPPC. ESR spectra of 16-PCSL, 16-SASL, and 16-MESL in DPPC multilamellar vesicles obtained at 34 °C. All spectra display a “shoulder” in the low-field and high-field lines, as indicated by the arrows.

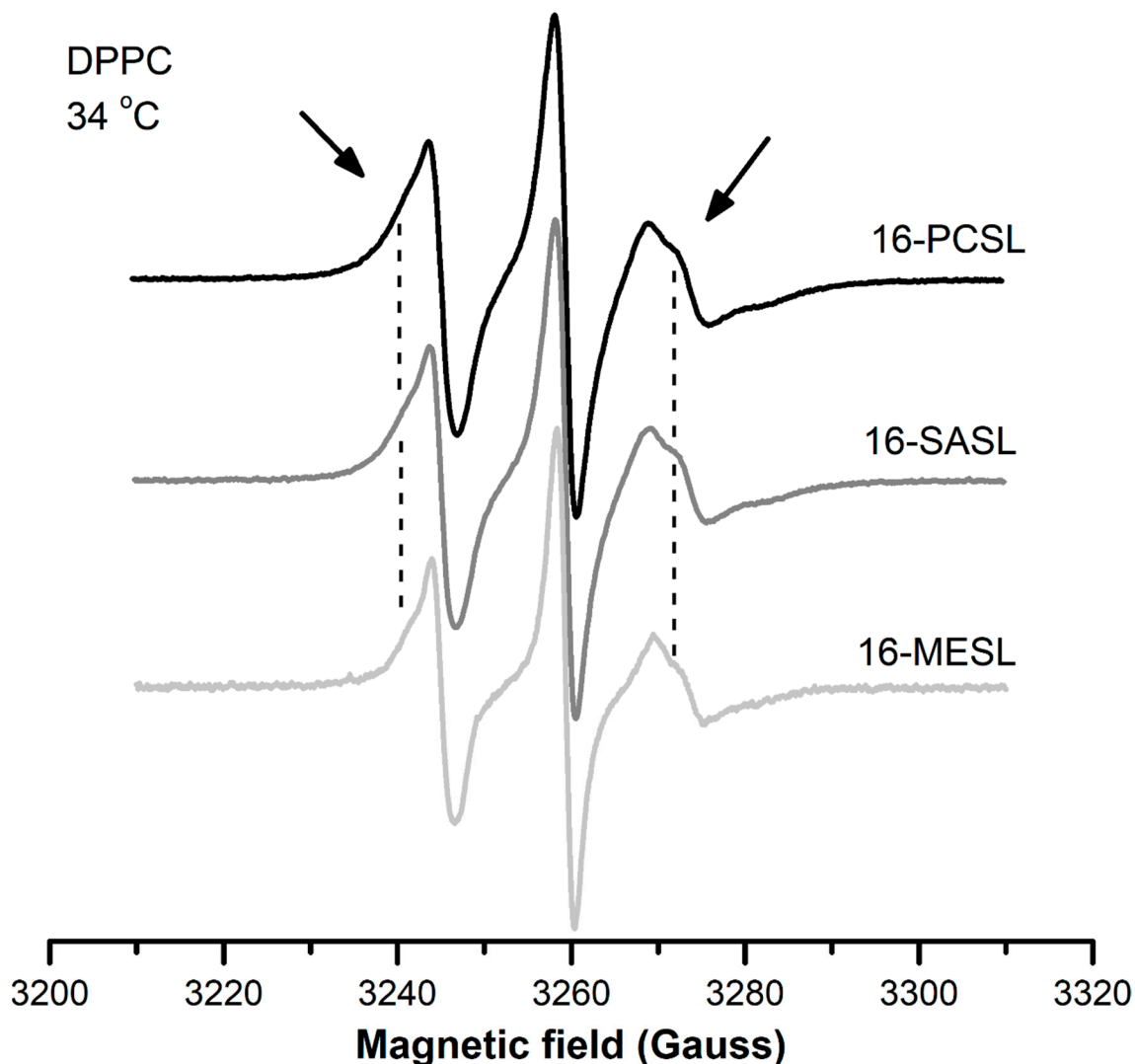


Figure S5: Experimental (black) and best-fit (red) ESR spectra of 16-PCSL in pure DPPC (**A** and **D**) and in DPPC/nicotine lipid vesicles at two concentrations: 2 mol% (**B** and **E**) and 10 mol% (**C** and **F**). Only representative spectra at selected temperatures are illustrated. The spectra in panels A, B and C were simulated with only one component, whereas those in panels D, E and F were fitted with two components (green and blue). Arrows point to the second component in the phase coexistence region.

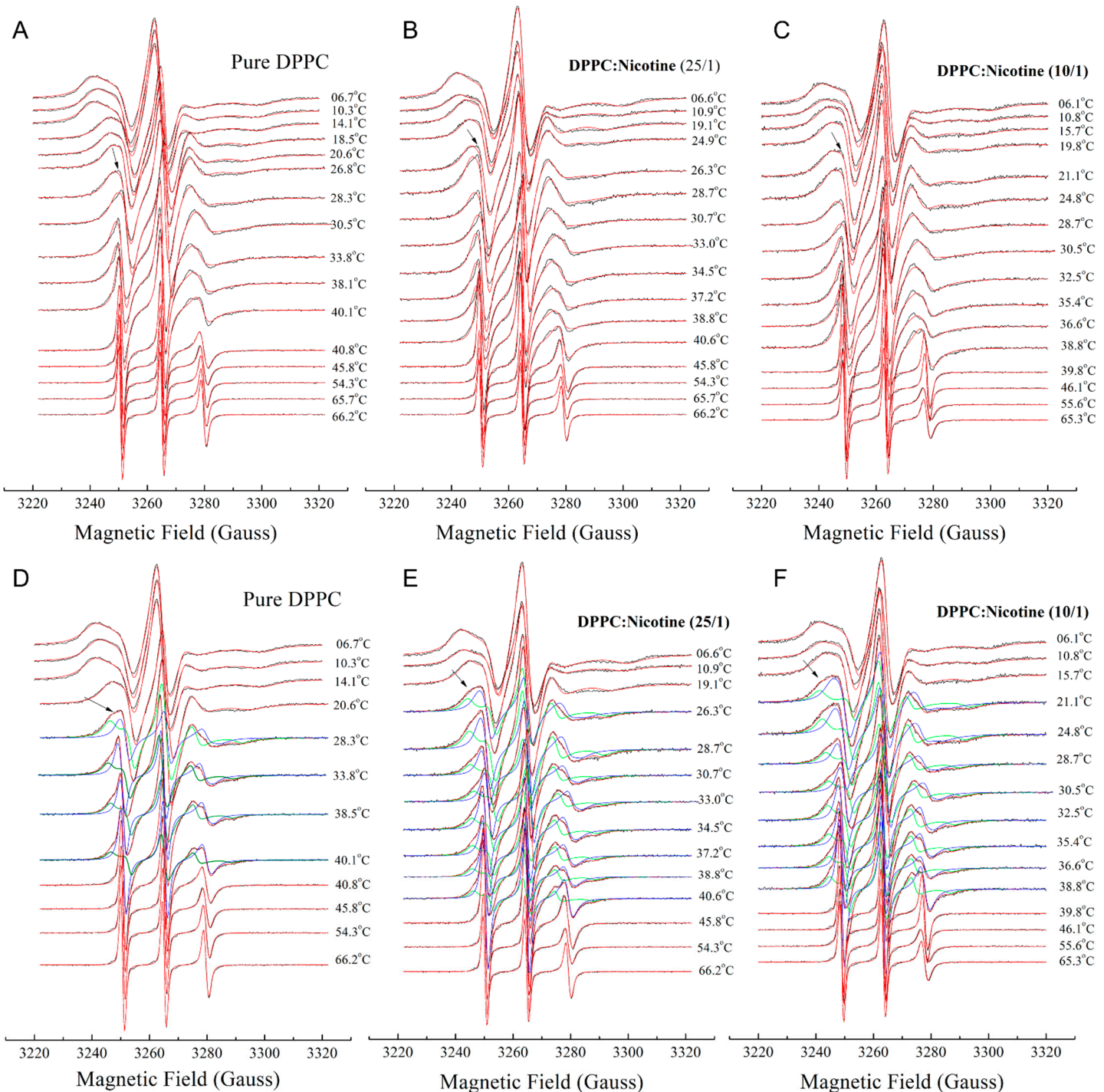


Figure S6: Effect of nicotine on the structural dynamics of the lipid headgroups.
 ESR spectra of DPPTC in (A) DPPC and (B) DPPC/POPC/POPG bilayers in the absence (black) and presence (red) of 10 mol% of nicotine. The spectra were obtained at the indicated temperatures and using a pH 7.4 buffer for DPPC and pH 7.4 and pH 5.0 buffers for the ternary lipid mixture.

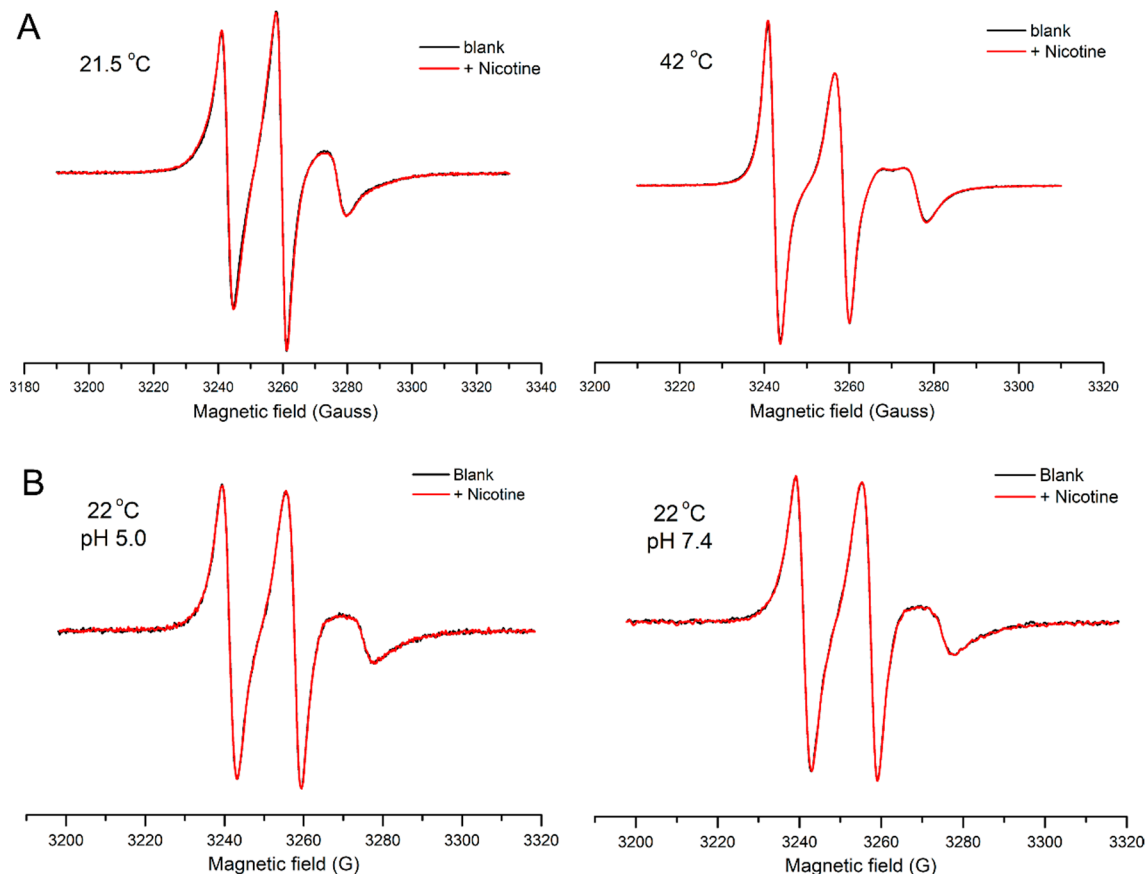


Figure S7: Entropy-enthalpy compensation of the nicotine-free and nicotine-containing pulmonary surfactant membrane models. (A) $T\Delta S \times \Delta H$ plots for pure DPPC (full squares) and DPPC/nicotine vesicles at two drug concentrations: 4 mol% (full triangles) and 10 mol% (empty diamonds). (B) $T\Delta S \times \Delta H$ plots for DPPC/POPC/POPG (full squares) and nicotine-enriched vesicles at different drug concentrations: 2 mol% (empty circles), 4 mol% (full triangles) and 10 mol% (empty diamonds).

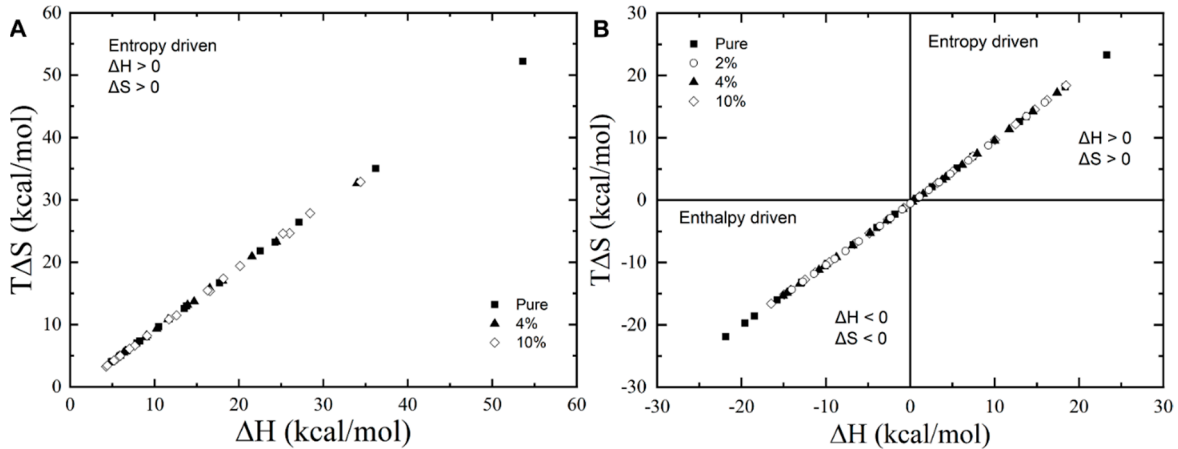


Figure S8. Membrane location of nicotine. MD snapshots showing the location and topology of neutral and monoprotonated nicotine molecules. Panels A and B depict the results for DPPC at 37 °C, panels C and D at 45 °C, while panels E and F represent the data for the lung surfactant model membrane (DPPC/POPC/POPG) at 37 °C. The numbers 1, 3, and 13 following the designation of each system on the top of the panels refer to the number of nicotine molecules in the system. Nicotine molecules are shown in cyan, with nitrogen atoms in blue; water molecules are shown in red, and the lipid bilayer is displayed with phospholipid phosphate atoms in orange spheres and tails in gray.

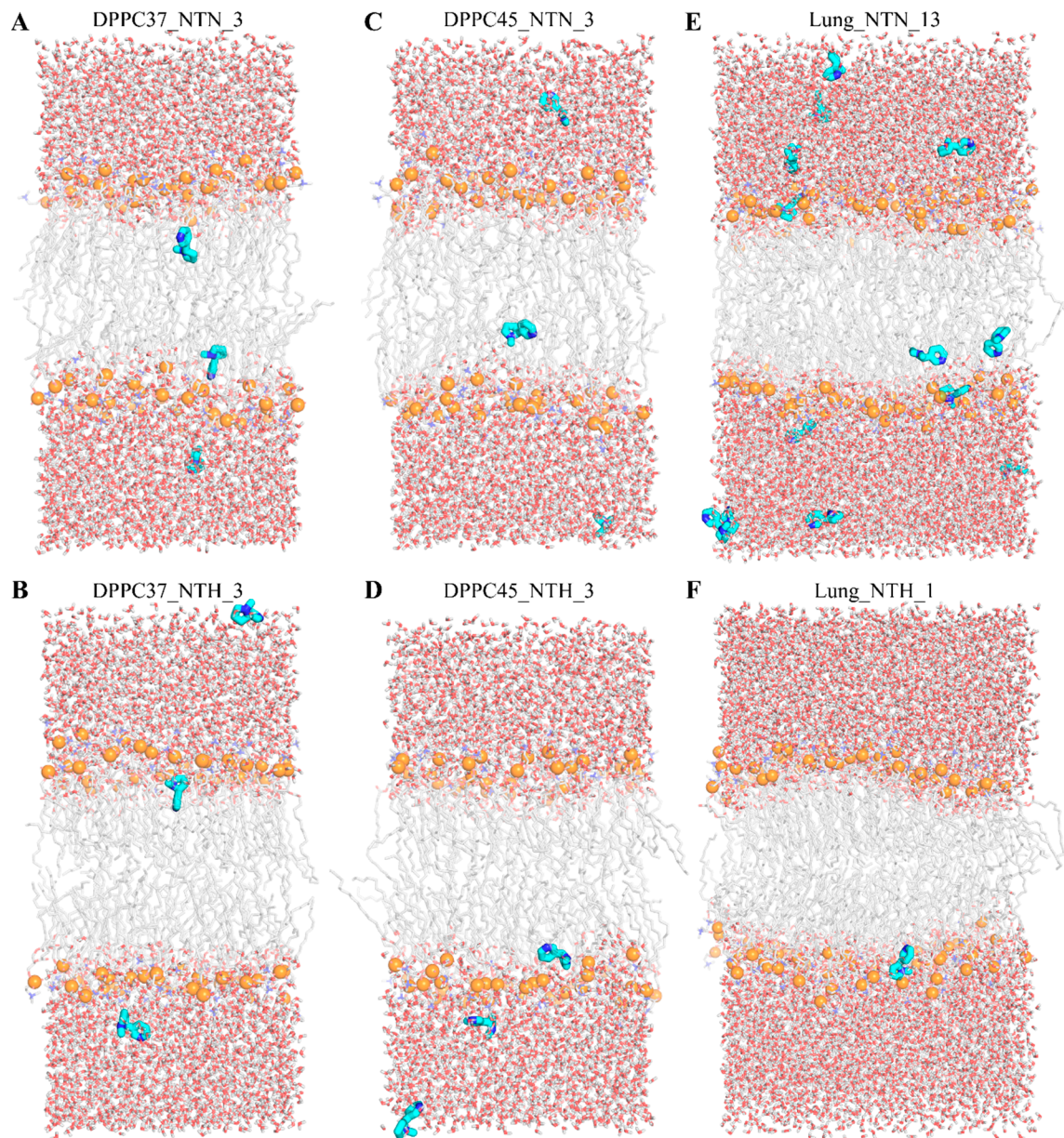


Figure S9: Time-dependent contacts, in percentage, between the protonated and neutral nicotine species with the other molecules (water, lipids, and nicotine) at different concentrations for DPPC at 37 °C. The contact is considered when the distance between any atom (including hydrogen) of two molecules is less than 3 Å. The numbers 1, 3, and 7 following the designation of each system on the top of the panels refer to the number of nicotine molecules in the system.

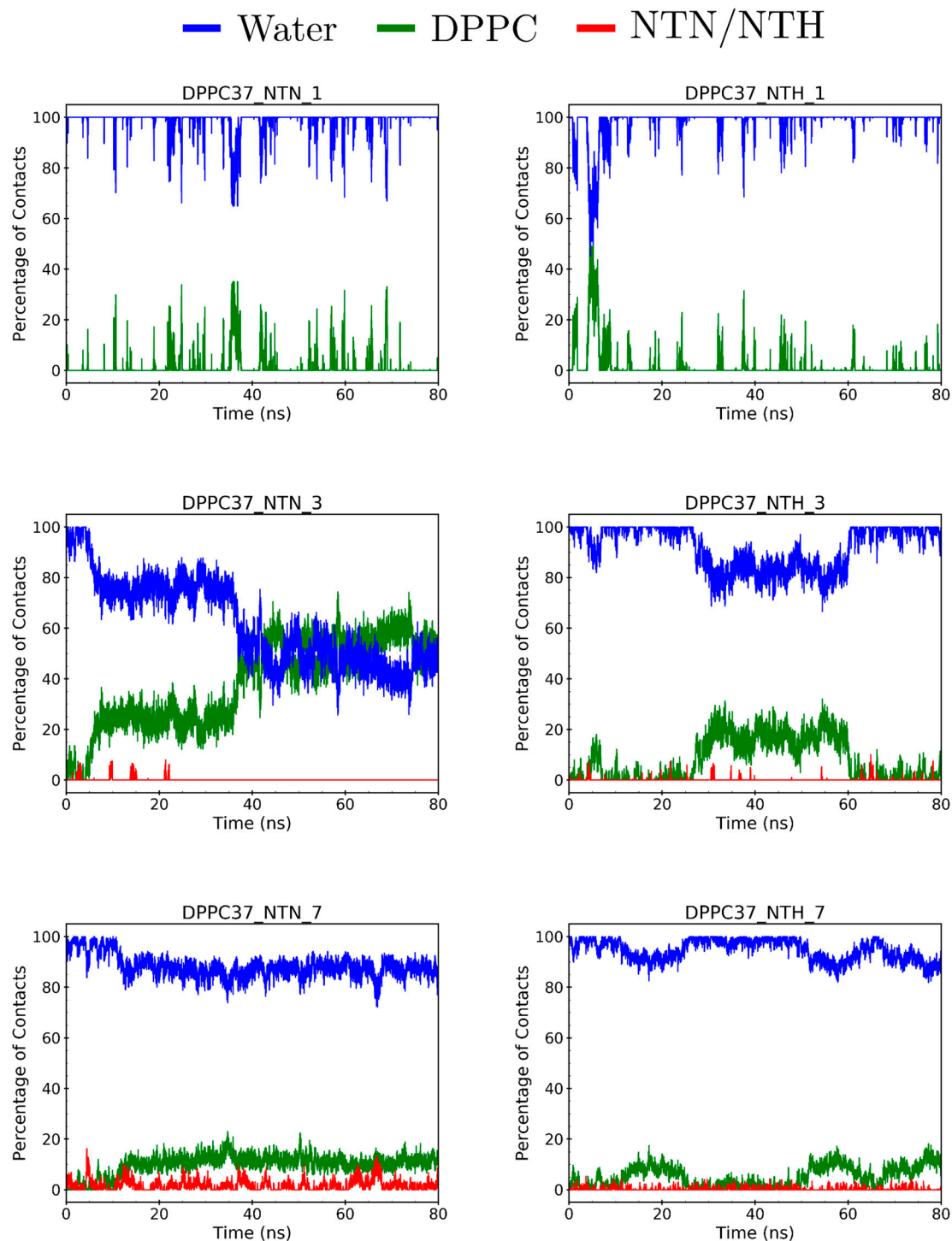


Figure S10: Time-dependent contacts, in percentage, between the protonated and neutral nicotine species with the other molecules (water, lipids, and nicotine) at different concentrations for DPPC at 45 °C. The contact is considered when the distance between any atom (including hydrogen) of two molecules is less than 3 Å. The numbers 1, 3, and 7 following the designation of each system on the top of the panels refer to the number of nicotine molecules in the system.

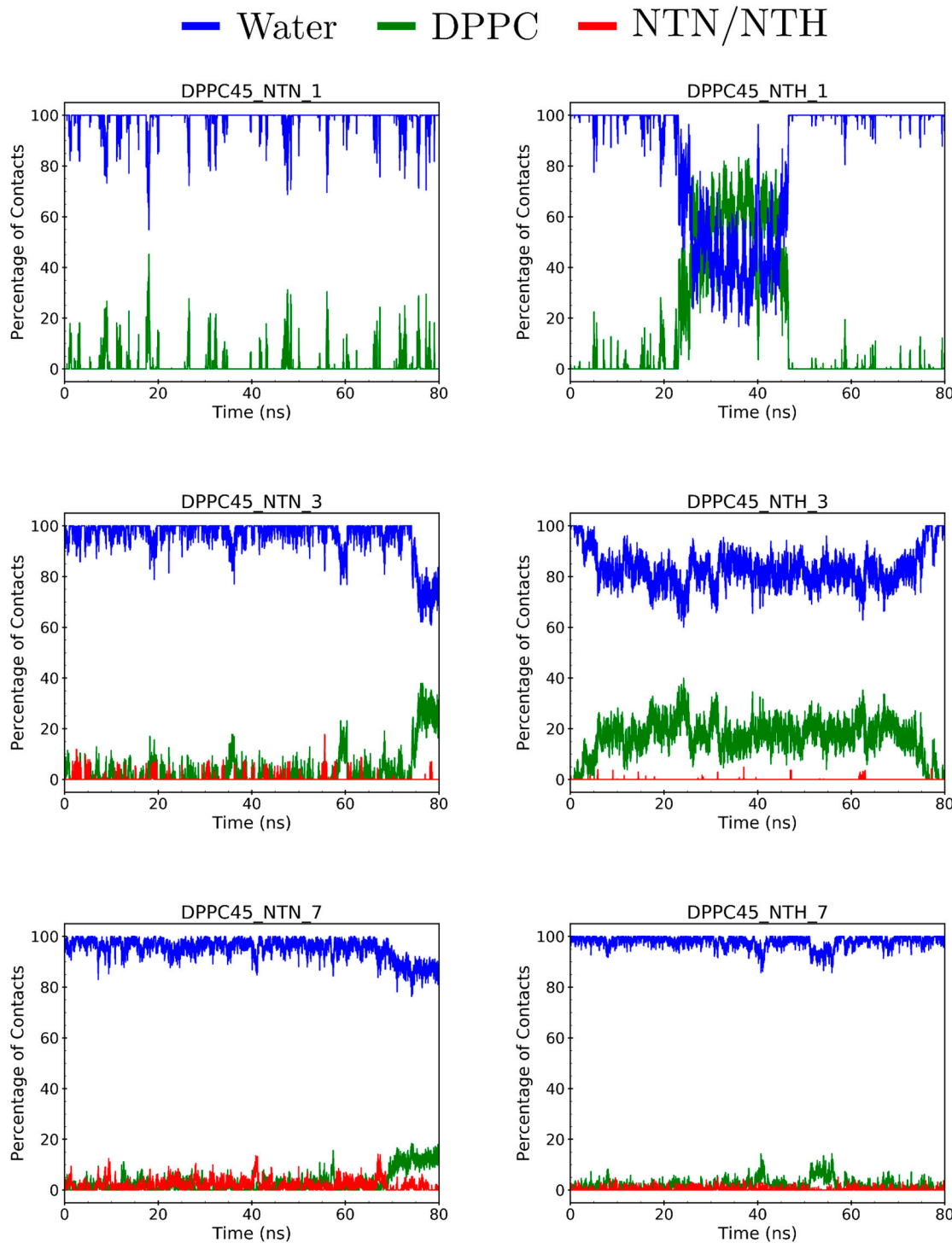


Figure S11: Time-dependent contacts, in percentage, between the protonated and neutral nicotine species with the other molecules (water, lipids, and nicotine) at different concentrations for DPPC/POPC/POPG (4:3:1 molar ratio) at 37°C. The contact is considered when the distance between any atom (including hydrogen) of two molecules is less than 3 Å. The numbers 1, 5, and 13 following the designation of each system on the top of the panels refer to the number of nicotine molecules in the system.

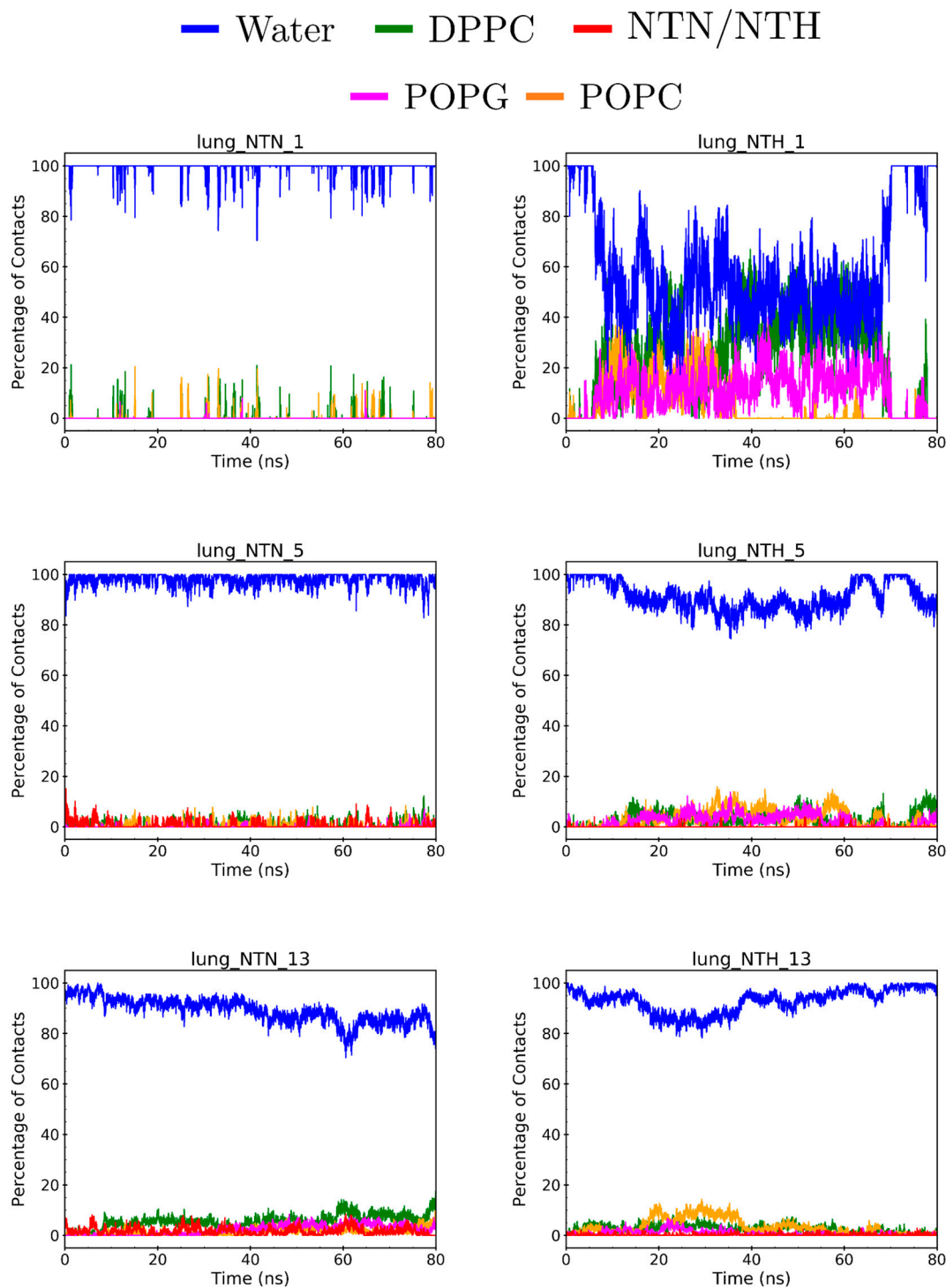


Table S1: Summary of the molecular dynamics simulation systems. The systems are identified by the membrane type (DPPC or lung), the nicotine protonation state (NTN for neutral or NTH for monoprotonated), the temperature (37 or 45 °C), and the number of nicotine molecules in the system.

System	Nicotine Protonation	Membrane Type	# of NTN or NTH	Temperature (K)
DPPC37_NTN_1	NTN	DPPC	1	310.15
DPPC37_NTN_3	NTN	DPPC	3	310.15
DPPC37_NTN_7	NTN	DPPC	7	310.15
DPPC37_NTH_1	NTH	DPPC	1	310.15
DPPC37_NTH_3	NTH	DPPC	3	310.15
DPPC37_NTH_7	NTH	DPPC	7	310.15
DPPC45_NTN_1	NTN	DPPC	1	318.15
DPPC45_NTN_3	NTN	DPPC	3	318.15
DPPC45_NTN_7	NTN	DPPC	7	318.15
DPPC45_NTH_1	NTH	DPPC	1	318.15
DPPC45_NTH_3	NTH	DPPC	3	318.15
DPPC45_NTH_7	NTH	DPPC	7	318.15
Lung_NTN_1	NTN	DPPC/POPC/POPG	1	310.15
Lung_NTN_5	NTN	DPPC/POPC/POPG	5	310.15
Lung_NTN_13	NTN	DPPC/POPC/POPG	13	310.15
Lung_NTH_1	NTH	DPPC/POPC/POPG	1	310.15
Lung_NTH_5	NTH	DPPC/POPC/POPG	5	310.15
Lung_NTH_13	NTH	DPPC/POPC/POPG	13	310.15

Table S2: Thermodynamic parameters associated with the 16-PCSL probe partitioned between the ordered and disordered phases of both DPPC and the lung surfactant model membranes at different lipid-to-drug molar ratios. The parameters were obtained by fitting the equation 2 to the experimental data up to the third order for DPPC vesicles, and to the second order for DPPC/POPC/POPG membranes.

Sample	a (x10 ²)	b x10 ⁵ (K)	c x10 ⁷ (K ²)	d x10 ¹² (K ³)
DPPC				
blank	397 ± 50	-367 ± 50	1120 ± 150	-1.1 ± 0.2
25:1	155 ± 20	-142 ± 20	433 ± 30	-0.4 ± 0.1
10:1	102 ± 50	-92 ± 5	277 ± 10	-0.3 ± 0.1
DPPC/POPC/POPG				
blank	532 ± 10	-302 ± 6	42.8 ± 0.8	—
50:1	344 ± 2	-196 ± 1	27.8 ± 0.2	—
25:1	357 ± 2	-203 ± 1	28.9 ± 0.2	—
10:1	415 ± 3	-235 ± 2	33.4 ± 0.3	—

Table S3: Partial charge assigned to NTN.

Atom name	Atom type	Charge
C	CA_0	0.456
H	H4	0.106
C1	CA	-0.267
C2	CA	0.084
H1	HA	0.117
C3	CA	-0.436
H2	HA	0.160
C4	CA	0.467
H3	H4	0.038
N	NB	-0.745
C5	C3	0.128
H4	H1	0.088
N1	N3	-0.693
C6	C3	0.012
H5	HC	0.029
H6	HC	0.029
C7	C3	-0.196
H7	HC	0.058
H8	HC	0.058
C8	C3	0.164
H9	H1	0.059
H10	H1	0.059
C9	C3	-0.027
H11	H1	0.084
H12	H1	0.084
H13	H1	0.084

Table S4: Parameters assigned to NTN.**A. BONDS**

Atom type	Kr	req
CA-CA	478.40	1.387
CA-NB	483.10	1.342
CA-H4	342.90	1.088
C3-CA	323.50	1.513
CA-HA	344.30	1.087
C3-N3	320.60	1.470
C3-C3	303.10	1.535
C3-H1	335.90	1.093
C3-HC	337.30	1092
HT_W-HT_W	0.00	1.514
OT_W-HT_W	450.00	0.957
CA_0-CA	478.40	1.387
CA_0-NB	483.10	1.342
CA_0-H4	342.90	1.088

B. ANGLES

Atom type	Kθ	θeq
CA-CA-CA	67.18	119.970
CA-CA-C3	63.84	120.630
CA-NB-CA	68.59	115.860
CA-CA-NB	69.16	122.630
CA-CA-H4	48.24	121.090
CA-CA-HA	48.46	120.010
CA-C3-N3	66.18	112.130
CA-C3-C3	63.25	112.090
CA-C3-H1	46.78	110.950
NB-CA-H4	51.82	115.940
C3-N3-C3	64.01	110.900
C3-C3-C3	63.21	110.630
C3-C3-HC	46.37	110.050
N3-C3-C3	66.18	110.380
N3-C3-H1	49.39	109.920
C3-C3-H1	46.36	110.070
HC-C3-HC	39.34	108.350
H1-C3-H1	39.18	109.550
HT_W-OT_W-HT_W	55.00	104.520
CA_0-CA-CA	67.18	119.970
CA_0-CA-C3	63.84	120.630
CA_0-NB-CA	68.59	115.860
CA-CA_A-NB	69.16	122.630
CA-CA_0-H4	48.24	121.090
NB-CA_0-H4	51.82	115.940

C. DIHEDRAL

Atom type	$k\phi$	n	δ
X-CA-CA-X	3.625	2	180.0
X-CA-NB-X	4.800	2	180.0
X-C3-CA-X	0.000	2	0.0
X-C3-N3-X	0.300	3	0.0
C3-C3-N3-C3	0.300	3	0.0
C3-C3-N3-C3	0.480	2	180.0
X-C3-C3-X	0.156	3	0.0
C3-C3-C3-C3	0.180	3	0.0
C3-C3-C3-C3	0.250	2	180.0
C3-C3-C3-C3	0.200	1	180.0
HC-C3-C3-C3	0.160	3	0.0
HC-C3-C3-HC	0.150	3	0.0
CA-CA-CA_0-NB	3.625	2	180.0
CA-CA-CA_0-H4	3.625	2	180.0
NB-CA_0-CA-C3	3.625	2	180.0
C3-CA-CA_0-H4	3.625	2	180.0
CA-CA_0-NB-CA	4.800	2	180.0
CA-NB-CA_0-H4	4.800	2	180.0
CA_0-CA-CA-CA	3.625	2	180.0
CA_0-CA-CA-HA	3.625	2	180.0
CA_0-CA-C3-N3	1.367	1	0.0
CA_0-CA-C3-N3	0.126	2	180.0
CA_0-CA-C3-N3	0.076	3	180.0
CA_0-CA-C3-N3	0.000	4	0.0
CA_0-CA-C3-N3	0.136	6	0.0
CA_0-CA-C3-C3	0.000	2	0.0
CA_0-CA-C3-H1	0.000	2	0.0
CA_0-NB-CA-CA	4.800	2	180.0
CA_0-NB-CA-H4	4.800	2	180.0

D. IMPROBERS

Atom type	K_ω	ω_0
CA-H4-CA-NB	1.100	180.0
C3-CA-CA-CA	1.100	180.0
X-X-CA-HA	1.100	180.0
CA-H4-CA_0-NB	1.100	180.0
C3-CA_0-CA-CA	1.100	180.0

E. NONBONDED

Atom type	ϵ	$\frac{R_{min}}{2}$	ϵ (for 1 - 4)	$\frac{R_{min}}{2}$ (for 1-4)
CA	-0.0860	1.9080	-0.0430	1.9080
NB	-0.1700	1.8240	-0.0850	1.8240
C3	-0.1094	1.9080	-0.0547	1.9080
N3	-0.1700	1.8240	-0.0850	1.8240
H4	-0.0150	1.4090	-0.0075	1.4090

HA	-0.0150	1.4590	-0.0075	1.4590	
H1	-0.0157	1.3870	-0.0078	1.3870	
HC	-0.0157	1.4870	-0.0078	1.4870	
HT_W	-0.0460	0.2245			
OT_W	-0.1521	1.7685			
CA_0	-0.0860	1.9080	-0.0430	1.9080	

Table S5: Partial charge assigned to NTH.

Atom name	Atom type	Charge
C	CA_0	0.271
H	H4	0.064
C1	CA	-0.186
C2	CA	0.020
H1	HA	0.142
C3	CA	-0.312
H2	HA	0.176
C4	CA	0.339
H3	H4	0.081
N	NB	-0.513
C5	C3	0.119
H4	HX	0.102
N1	N4	-0.258
H5	HN	0.325
C6	C3	-0.129
H6	HC	0.090
H7	HC	0.090
C7	C3	-0.078
H8	HC	0.077
H9	HC	0.077
C8	C3	0.064
H10	HX	0.086
H11	HX	0.086
C9	C3	-0.045
H12	HX	0.104
H13	HX	0.104
H14	HX	0.104

Table S6: Parameters assigned to NTH.**A. BONDS**

Atom type	Kr	req
CA-CA	478.40	1.387
CA-NB	483.10	1.342
CA-H4	342.90	1.088
C3-CA	323.50	1.513
CA-HA	344.30	1.087
C3-N4	293.60	1.499
C3-C3	303.10	1.535
C3-HX	338.70	1.091
HN-N4	369.00	1.033
C3-HC	337.30	1.092
HT_W-HT_W	0.00	1.514
OT_W-HT_W	450.00	0.957
CA_0-CA	478.40	1.387
CA_0-NB	483.10	1.342
CA_0-H4	342.90	1.088

B. ANGLES

Atom type	Kθ	θeq
CA-CA-CA	67.18	119.970
CA-CA-C3	63.84	120.630
CA-NB-CA	68.59	115.860
CA-CA-NB	69.16	122.630
CA-CA-H4	48.24	121.090
CA-CA-HA	48.46	120.010
CA-C3-N4	64.87	114.540
CA-C3-C3	63.25	112.090
CA-C3-HX	46.69	111.440
NB-CA-H4	51.82	115.940
C3-N4-C3	62.84	110.640
C3-N4-HN	46.19	110.110
C3-C3-C3	63.21	110.630
C3-C3-HC	46.37	110.050
N4-C3-C3	64.45	114.320
N4-C3-HX	49.02	107.910
C3-C3-HX	46.02	111.740
HC-C3-HC	39.34	108.350
HX-C3-HX	39.04	110.740
HT_W-OT_W-HT_W	55.00	104.520
CA_0-CA-CA	67.18	119.970
CA_0-CA-C3	63.84	120.630
CA_0-NB-CA	68.59	115.860
CA-CA_A-NB	69.16	122.630
CA-CA_0-H4	48.24	121.090
NB-CA_0-H4	51.82	115.940

C. DIHEDRAL

Atom type	$k\phi$	n	δ
X-CA-CA-X	3.625	2	180.0
X-CA-NB-X	4.800	2	180.0
X-C3-CA-X	0.000	2	0.0
X-C3-N4-X	0.156	3	0.0
X-C3-C3-X	0.156	3	0.0
C3-C3-C3-C3	0.180	3	0.0
C3-C3-C3-C3	0.250	2	180.0
C3-C3-C3-C3	0.200	1	180.0
HC-C3-C3-C3	0.160	3	0.0
HC-C3-C3-HC	0.150	3	0.0
CA-CA-CA_0-NB	3.625	2	180.0
CA-CA-CA_0-H4	3.625	2	180.0
NB-CA_0-CA-C3	3.625	2	180.0
C3-CA-CA_0-H4	3.625	2	180.0
CA-CA_0-NB-CA	4.800	2	180.0
CA-NB-CA_0-H4	4.800	2	180.0
CA_0-CA-CA-CA	3.625	2	180.0
CA_0-CA-CA-HA	3.625	2	180.0
CA_0-CA-C3-N4	0.482	1	0.0
CA_0-CA-C3-N4	0.778	2	0.0
CA_0-CA-C3-N4	0.143	3	180.0
CA_0-CA-C3-N4	0.260	4	0.0
CA_0-CA-C3-N4	0.273	6	0.0
CA_0-CA-C3-C3	0.000	2	0.0
CA_0-CA-C3-HX	0.000	2	0.0
CA_0-NB-CA-CA	4.800	2	180.0
CA_0-NB-CA-H4	4.800	2	180.0

D. IMPROBERS

Atom type	K_ω	ω_0
CA-H4-CA-NB	1.100	180.0
C3-CA-CA-CA	1.100	180.0
X-X-CA-HA	1.100	180.0
CA-H4-CA_0-NB	1.100	180.0
C3-CA_0-CA-CA	1.100	180.0

E. NONBONDED

Atom type	ε	$\frac{R_{min}}{2}$	ε (for 1 - 4)	$\frac{R_{min}}{2}$ (for 1-4)
CA	-0.0860	1.9080	-0.0430	1.9080
NB	-0.1700	1.8240	-0.0850	1.8240
C3	-0.1094	1.9080	-0.0547	1.9080
N3	-0.1700	1.8240	-0.0850	1.8240
H4	-0.0150	1.4090	-0.0075	1.4090
HA	-0.0150	1.4590	-0.0075	1.4590
HX	-0.0157	1.1000	-0.0078	1.1000

HN	-0.0157	0.6000	-0.0078	0.6000	
HC	-0.0157	1.4870	-0.0078	1.4870	
HT_W	-0.0460	0.2245			
OT_W	-0.1521	1.7685			
CA_0	-0.0860	1.9080	-0.0430	1.9080	

References

1. Basso, L.G.M.; Rodrigues, R.Z.; Naal, R.M.Z.G.; Costa-Filho, A.J. Effects of the Antimalarial Drug Primaquine on the Dynamic Structure of Lipid Model Membranes. *Biochim Biophys Acta Biomembr* **2011**, *1808*, 55–64, doi:10.1016/j.bbamem.2010.08.009.
2. Clayton, P.M.; Vas, C.A.; Bui, T.T.T.; Drake, A.F.; McAdam, K. Spectroscopic Investigations into the Acid–Base Properties of Nicotine at Different Temperatures. *Analytical Methods* **2012**, *5*, 81–88, doi:10.1039/C2AY25678A.